

# Charge Transfer Inefficiency in the Hubble Space Telescope since Servicing Mission 4

Richard Massey

Royal Observatory, Blackford Hill, Edinburgh EH9 3HJ

Accepted —. Received —; in original form —

## ABSTRACT

We update a physically-motivated model of radiation damage in the *Hubble Space Telescope* Advanced Camera for Surveys/Wide Field Channel, using data up to mid 2010. We find that Charge Transfer Inefficiency increased dramatically before shuttle Servicing Mission 4, with  $\sim 1.3$  charge traps now present per pixel. During detector readout, charge traps spuriously drag electrons behind all astronomical sources, degrading image quality in a way that affects object photometry, astrometry and morphology. Our detector readout model is robust to changes in operating temperature and background level, and can be used to iteratively *remove* the trailing by pushing electrons back to where they belong. The result is data taken in mid-2010 that recovers the quality of imaging obtained within the first six months of orbital operations.

**Key words:** space vehicles — instrumentation: detectors — methods: data analysis

## 1 INTRODUCTION

The harsh radiation environment above the Earth’s atmosphere gradually degrades all electronic equipment, including the sensitive Charge-Coupled Device (CCD) imaging detectors used in the *Hubble Space Telescope* (HST) Advanced Camera for Surveys (ACS)/Wide Field Channel (WFC). The detectors work by collecting photoelectrons in a potential well at each pixel. At the end of an exposure, these electrons are then transferred, row by row, to an amplifier at the edge of the device, where they are counted. However, radiation damage to the silicon lattice creates charge traps that temporarily capture electrons and release them only after a characteristic delay. Any electrons captured during the transfer to the readout register can reemerge, several pixels later, as a spurious “Charge Transfer Inefficiency” (CTI) trail behind every bright source.

CTI trailing is particularly troublesome because the amount of flux trailed is a nonlinear function of the flux, size and shape of a source. The effect is therefore *not* a convolution. A multitude of ad-hoc schemes have been invented to estimate (and subtract) the effect of CTI from catalogues of object photometry, astrometry and shape (*e.g.* Chiaberge *et al.* 2009; Cawley *et al.* 2002; Rhodes *et al.* 2007). However, since CTI moves electrons around fairly predictably at the image level, the ideal approach for correction is to directly shuffle those electrons back to where they belong. Since detector readout is the last process to happen during data acquisition, this can be conveniently carried out as the first process in data processing. While no algorithm can undo the nonlinear movement of electrons in a sin-

gle step, Bristow (2003a) and Piatek *et al.* (2005) proposed an iterative algorithm to remove trailing by repeatedly (re-)adding new trailing. This requires a model of the (forward) readout process. A physically-motivated model was developed for ACS/WFC by Massey *et al.* (2010), using measurements from trails behind warm pixels in science imaging.

This letter updates the Massey *et al.* (2010) CCD readout model and pixel-based CTI correction. In §2, we account for an additional species of charge trap with a long characteristic release time, and measure the density of traps in the detector up to mid-2010. In §3, we implement the improved CTI correction algorithm and evaluate its performance. In §4, we discuss the overall performance of the detectors, in light of changes to their operational temperature and the long period during which they were offline.

## 2 UPDATED CCD READOUT MODEL

### 2.1 Well filling rate

We use a “volume-driven” CCD readout model, whose first ingredient is the rate at which electrons fill up the potential well in a pixel. A cloud of  $n_e$  electrons grows in size as electrons are added, and a cloud with a larger cross-sectional area will be exposed to more charge traps when it is swept through the silicon lattice during readout. As first suggested by Biretta & Kozhurina-Platais (2005), if the traps are uniformly distributed in 3D, the well filling rate can be measured using hot pixels (which would appear as isolated  $\delta$ -functions in the absence of radiation damage) in

arXiv:1009.4335v1 [astro-ph.IM] 22 Sep 2010

ordinary, on-orbit imaging – from the increasing fraction of electrons trailed behind increasingly warm pixels. Universally, the fraction of trailed electrons is greatest for faint sources, demonstrating that the size of the cloud grows more slowly than the number of electrons. This crucial point explains why CTI is nonlinear.

Massey *et al.* (2010) parameterised the height  $h(n_e)$  of a cloud as zero for the first  $d \approx 100$  electrons, then increasing as  $h \propto (n_e - d)^\alpha$  where  $\alpha \approx 0.58$ . The first electrons were assumed to reside in a supplementary buried channel or “notch” specifically intended to compress their volume and minimise the degradation of very faint sources. The notch is created by doping the silicon lattice, but HST engineers now believe that the initial atomic implant in the ACS/WFC detectors was unstable and has diffused (Linda Smith, priv. comm. 2010). If this were true, it would result in trailing behind even faint sources. The interpretation of our (updated) measurements of faint in science images is hindered by the zodiacal sky background, but the data are consistent with no notch. Anderson & Bedin (2010) studied warm pixels in dark exposures, which have less noise, and confirmed trails behind warm pixels containing as few as  $\sim 20$  electrons. We shall therefore adopt a model in which the notch is no longer operational  $d \equiv 0$ . Strictly, we should model the gradual disappearance of the notch over time – but the same sky background that makes it difficult to measure this effect also hides real science data from its influence.

The profiles of CTI trails in dark exposures are reproduced from Anderson & Bedin (2010) in figure 1. The relative fraction of electrons trailed behind increasingly warm pixels confirms that  $\alpha \approx 0.57$ . However, when ignoring a notch, measurements from science images like those in Massey *et al.* (2010) (see §2.3) prefer  $\alpha = 0.465 \pm 0.016$  both before and after Servicing Mission 4. The effect of this parameter is apparent as the difference between the data and the solid grey curves of figure 1, which show the Massey *et al.* (2010) prediction but using the lower value of  $\alpha$ . For very hot pixels, the first  $\sim 10$  pixels of the predicted trail are within 3% of the Anderson & Bedin (2010) data (*c.f.* the best-fit dashed curve) – an impressive agreement considering these measurements are completely independent. However, predictions of the relative trail heights begin to disagree when the model is extrapolated down towards faint trails. Since the measurements of these faint trails are affected by a complex interaction with the sky background, we adopt our measurement of  $\alpha = 0.465$  because its origin is closest to the data we will eventually want to correct.

## 2.2 Charge trap species

The second ingredient of a CCD readout model is the density and characteristic release times of charge traps. Shockley-Read & Hall theory of solid-state devices (*e.g.* Hardy 1998; Janesick *et al.* 2001) suggests that we can expect several distinct species of traps at a variety of energies  $\Delta E$  below the band gap, all of which capture charge almost instantly then release it with a probabilistic delay governed by an exponential  $e^{-t/\tau}$ . The characteristic release time  $\tau$  depends upon operating temperature as  $\tau \propto T^{-2} e^{\Delta E/kT}$ .

In early ACS data, Massey *et al.* (2010) found two species of traps with characteristic release times  $\tau =$

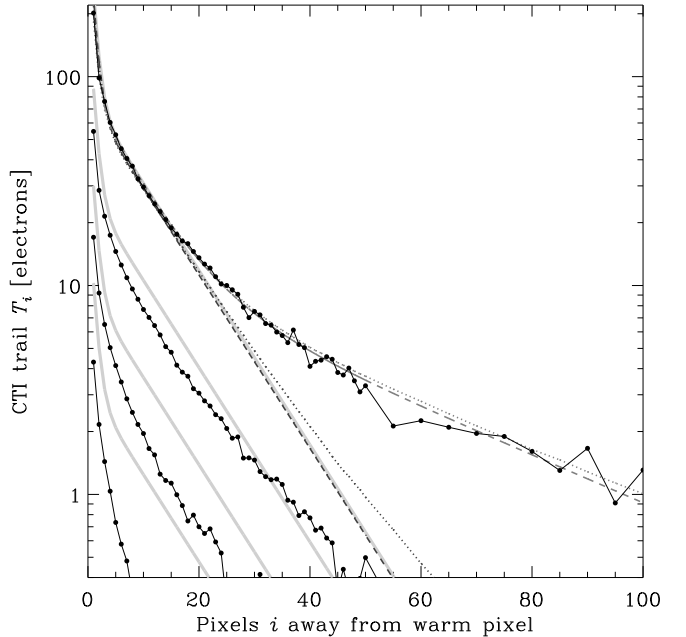


**Figure 1.** CTI trailing behind warm pixels in dark exposures. Black points reproduce the measurements from figure 5 of Anderson & Bedin (2010), for warm pixels at least 1500 pixels from the readout register and containing approximately 20, 200, 2000 and 20000 electrons (bottom to top). Solid grey lines show predictions of the Massey *et al.* (2010) model, which used only the first 9 pixels behind warm pixels, and has had to be extrapolated down to the lower trails. The agreement between these completely independent analyses is impressive. Dashed lines show best-fit models of the trail behind the brightest curve (which is most reliably measured), using a double exponential (with the decay times of Massey *et al.* 2010) and a triple exponential with free parameters. The dotted lines add secondary electron capture to the calculation, whereby trailed electrons can be recaptured and retrailed. This represents the difference between our full algorithm and the (much faster) approximation of Anderson & Bedin (2010).

$\{0.88, 10.4\}$  multiplied by the  $3212\mu\text{s}$  CCD clocking speed, and associated them with impure E-centre complexes at  $\Delta E = 0.31$  and  $0.34$  eV (Hopkinson 2001). The trap species were present in a density ratio of 1 : 3.

In July 2006, the operating temperature of the WFC detectors was lowered from  $-77\text{C}$  to  $-81\text{C}$  (Sirianni, Gilliland & Sembach 2006; Mack *et al.* 2007). Anderson & Bedin (2010) modelled the trail profiles in subsequent imaging using an empirical look-up table. However, the smooth curves overlaid on their data in figure 1 demonstrate that the profiles can still be accurately fit using multiple exponentials. The steep dashed line shows a two-species Massey *et al.* (2010) prediction. The more extended dashed line shows the best-fit three-species model in which both the trap densities and release times are allowed to vary. This analysis yields trap release times of  $\tau = \{0.74 \pm 0.55, 7.7 \pm 4.3, 37 \pm 33\} \times 3212\mu\text{s}$  with amplitudes of  $\{0.18 \pm 0.10, 0.61 \pm 0.3, 0.51 \pm 0.26\}$  traps exposed to the 20,000 electron charge cloud – *i.e.* a ratio of 1 : 3.38 : 2.85.

Pure E-centre complexes  $0.44$  eV below the conduction band are expected to produce the next-longest trails, with  $\tau \sim 180 \times 3212\mu\text{s}$  (Jones 2000). This is longer than measured,

but the discrepancy may be due to degeneracies in the fitting of decaying exponentials. This is a notoriously difficult task because the exponentials become more and more similar to a constant as they get longer. Our measurement of long trails is even more difficult because the sky background is noisy and its subtraction is uncertain. However, the degeneracy of exponentials also means that our trails can be successfully fitted with different  $\tau$  (and even an additional trap species) by simply adjusting their normalisations. We therefore adopt the superior three-trap model, with the fitted parameters after July 2006 and, assuming that the third species are indeed pure E-centres, we update the pre-July 2006 values to  $\tau = \{0.48, 4.86, 20.6\} \times 3212\mu\text{s}$ .

### 2.3 Charge trap density

As in Massey *et al.* (2010), we measure the effective trap density from the amount of trailing in the first nine pixels behind warm pixels in archival HST imaging. Large extragalactic surveys prove most useful to build up a uniform dataset extending over a long period of time, and to isolate the warm pixels from crowding by real astronomical sources. To span the entire lifetime of ACS, we gather data from HST programmes GO-9075 and GO-10496 (PI: Saul Perlmutter), GO-9822 and GO-10092 (PI: Nick Scoville), GO-10896 (PI: Paul Kalas), GO-11563 (PI: Garth Illingworth) and GO-11600 (PI: Benjamin Weiner). The first four of these were observed using a commanded gain setting of 1 and the last three with a setting of 2; these are distinguished as grey and black data points respectively in figure 2. The exposure time and filters – hence the background level – also vary between programmes.

Up to July 2006, we find that the total effective charge trap density increases linearly over time<sup>1</sup>. The trap density extrapolates back to a value at launch of a remarkably low value of  $\rho_q = 0.014 \pm 0.04$  per pixel. These manufacturing and process traps were dominated within less than two months by radiation-induced traps, which were created in orbit at a rate of  $(3.60 \pm 0.26) \times 10^{-4}$  per day.

After July 2006, the traps themselves continued to accumulate at a rate of  $(4.77 \pm 2.76) \times 10^{-4}$  per day. Lowering the operating temperature and lengthening the trails immediately reduced the amount of spurious flux in the first nine pixels by 22%. According to our model, however, the same amount of flux was lost, but it was just moved further. The continuity of the apparent trap density around this time, through changes in operating temperature, background level and default gain settings, provide a strong vindication of our model. Overall, the total trap density until January 2007 is well fit by  $\rho_q = (0.50 \pm 0.018) + (t - 1359) (3.55 \pm 0.22) \times 10^{-4}$  per pixel, where  $t$  is the number of days after 1 March 2002.

Since January 2007, degradation has been more rapid. Because of the long period when ACS was offline, it is not clear exactly when this damage accrued. It is quite possible that the radiation exposure simply increased. The solar cycle maximum ended around 2006, and the density of charged particles in low Earth orbit counterintuitively *increases* during solar minimum (Sirianni & Mutchler 2006). However,

even though our data suggest the rate of trap creation increased slightly in late 2006, it appears to have slowed again since 2009. A more likely scenario is that the damage built up abruptly while ACS was offline and warm, before shuttle Servicing Mission 4. The subsequent trap density is best-fit by  $\rho_q = (1.25 \pm 0.020) + (t - 2873) (2.93 \pm 2.25) \times 10^{-4}$ /pixel.

### 2.4 Algorithmic development

Anderson & Bedin (2010) and Short *et al.* (2010) ingeniously invoke a first-order symmetry of the readout process to increase the speed of the readout (and correction) algorithm. Electrons beginning 2048 pixels from the readout register undergo this many pixel-to-pixel transfers during readout. Each time, electrons may be captured or released by charge traps but, if the number of free electrons is high and the density of traps is small, every transfer is statistically similar. The fast algorithm performs only one transfer for each cloud of electrons, then multiplies its effect by the number of transfers it will see. This can be implemented quickly in practice by sweeping one pixel's worth of traps up the CCD (rather than all the electrons down the CCD). This approach is very powerful: we confirm that it decreases runtime by a factor of  $\sim 1000$  and even still allows for secondary charge capture, whereby a trailed electron can be subsequently recaptured and retrailed.

The limitation of this algorithm is that all of the capture (and recapture) of electrons is implemented at the level appropriate to the size of the electron cloud in the raw image. In the real readout process, as electrons are gradually removed from an image peak, the electron cloud shrinks and fewer are subsequently captured. Similarly, as electrons build up in a trail, the cloud grows and becomes exposed to more traps. This effect is illustrated as the difference between the dashed and solid lines in figure 1 and is most severe for faint sources – from which the fast algorithm even makes it possible to trail more electrons than are available. We propose a compromise between speed and accuracy by using one transfer to represent the first  $n_t$  transfers, then performing a new transfer to represent the next  $n_t$  and so on. Thus the height of local maxima slowly reduces and the height of trails slowly increases. We find that  $n_t = 140$  still provides a factor of  $\sim 70$  speedup, while producing a trailed image within 1 electron of that produced by the full algorithm everywhere on the detector for model parameters appropriate in early 2010.

Only one iteration of the Bristow (2003a) algorithm (see table 1 in Massey *et al.* 2010) was required to correct the circa 2004 COSMOS survey. This was because the low density of charge traps implied only a small, perturbative correction. To correct more recent data, Anderson & Bedin (2010) implemented five iterations. To qualitatively justify the number of iterations, it is merely necessary to test for convergence by calculating the difference to the corrected image after each step. Typical science images from early 2010 change by only one electron in a handful of pixels after three iterations, and by less than an electron in every pixel after four. Since each iteration has a large price in run time, we shall henceforth stop at the third iteration.

<sup>1</sup> Massey *et al.* (2010) demonstrated that monthly annealings do not reduce the effective trap density, so we also ignore them here.

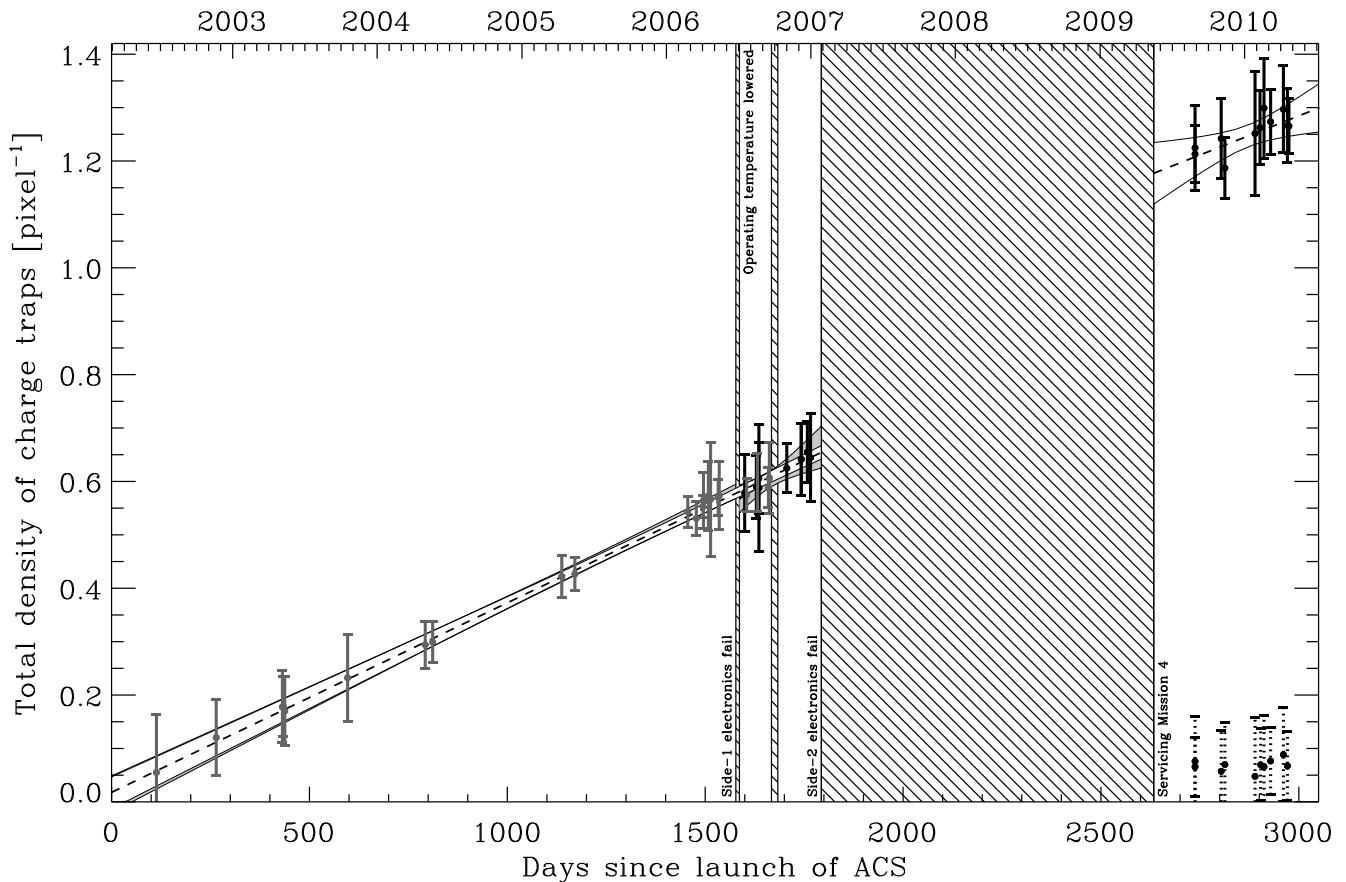


**Figure 2.** Measured density of charge traps in the ACS/WFC detectors, as they have accumulated over the lifetime of the camera. Measurements assume three trap species in a ratio of 1 : 3.38 : 2.85, with characteristic release times as described in the text. Grey (black) points indicate survey imaging acquired with a commanded gain setting of 1 (2), and all errors are  $1\sigma$ . Separate fits are shown to data before and after shuttle Servicing Mission 4, plus (noisier) fits to shorter periods in grey. Hatched regions indicate times when ACS was offline. Points with dotted error bars show the total absolute density of traps after correction.

### 3 IMAGE CORRECTION

We use our updated CCD readout model to correct science imaging throughout the lifetime of ACS, following the same procedure as Bristow (2003a). The points with dotted error bars in figure 2 show the effective density of charge traps after correction, which are a factor of 20 lower than in the raw data and consistent with image quality in the first six months of operations. For the sake of clarity, equivalent post-correction measurements are not shown for earlier epochs, but these recover about the same factor of 10-15 correction seen in Massey *et al.* (2010). Thus, ironically, as the CTI has got worse, the trailing has become easier to measure and the correction has become more accurate!

Figure 3 shows a region of a typical exposure, which was intentionally *not* used when measuring parameters of the readout model. The charge trailing that is now readily apparent in visual inspection of recent ACS images is successfully removed by our correction scheme.

### 4 DISCUSSION

We have developed a physically-motivated model of the readout and Charge Transfer Inefficiency (CTI) in the ACS/WFC detectors throughout their lifetime. We find that

there are approximately 1.3 charge traps per pixel in mid-2010, split between three different species. The extended trails produced by these traps can be accurately modelled as a sum of three decaying exponentials. We also used our model to correct images, reducing the amount of trailing by a factor of  $\sim 20$ , to a level seen in the first six months of orbital operations. As with Chiaberge *et al.* (2009), we still find no evidence for significant serial CTI (trailing perpendicular to the main trails, created by charge traps in the serial readout register), and therefore ignore this effect.

When building our model, we adopted the best available measurements from science imaging (which we performed) and dark exposures (from Anderson & Bedin 2010). The dark exposures were particularly useful to constrain the extended shape of trails out to  $\sim 100$  pixels and thus provide better correction of object photometry (Rhodes *et al.* 2010). Where measurements disagreed, the data's support for our physical model encouraged us to first extrapolate measurements obtained in the most reliable regime.

Removing the final few percent of CTI trails might require detailed investigation of such disagreements. In particular, there is mounting evidence that trails behind sources of different flux may change in *shape* as well as amplitude. A slight steepening of faint trail was also present in Massey *et al.* (2010), but ascribed to uncertain background level and read noise. Read noise is added to an image *after*

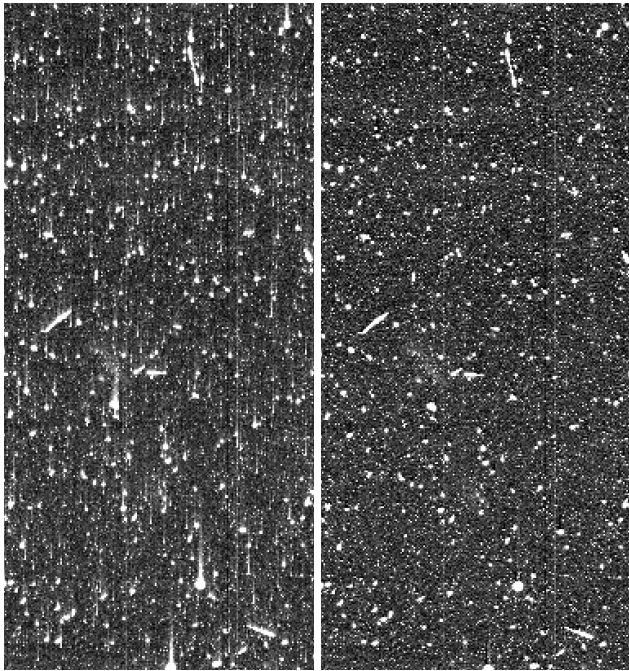


**Figure 3.** A typical raw ACS/WFC science exposure from early 2010 (HST-GO-11689, PI: Renato Dupke) before (left) and after (right) CTI correction. The  $380 \times 820$  pixel area selected is furthest on the detector from the readout register, and the logarithmic colour scale is chosen intentionally to highlight the CTI trails.

CTI, so creates spurious faint peaks that are not trailed, and act to spuriously steepen the true mean trail when they are accidentally included in the average. A physical effect that we do not model, but which might also affect faint trails, is the breakdown of the volume-driven charge packet model at very low flux levels discussed by Short *et al.* (2010). However, while this is important in Time-Delay Integration (TDI) mode observations (and potentially dark exposures), it is not so in science imaging where a large zodiacal sky background is always present. If anything, the effect would also predict shallower trails behind faint sources, from high- $\tau$  traps. A second physical mechanism by which the trail could change shape could be the onset of surface full well traps above a certain flux. However, this explanation seems unlikely at a value of 20,000 electrons (*c.f.*  $> 80,000$  full well depth), and because such traps would have been present since manufacture, while almost all appear to have accumulated over time at the same rate. We shall therefore continue to use a single trail profile, but recommend further testing of this apparent shape change, for example in combination with mean-variance measurements at a range of flux levels to determine whether the shape change is gradual or discreet and, if discreet, whether it coincides with other discontinuities.

The 4C decrease in the operating temperature of the ACS/WFC detectors in July 2006 did not affect the density of charge traps, or the amount of flux lost from a source. However, it lengthened their release times and the amount of spurious flux in the first 9 pixels behind a source fell by 22%, which benefits some astronomical measurements. Weak lensing measurements suffer by way of a spurious shear

signal induced the readout direction. Extrapolating from the trap characterisation of Rhodes *et al.* (2010), we estimate in mid-2010 a mean shear of  $\sim 5\%$  in galaxies detected at a S/N of 10. Similarly, we expect a value twice as bad for a galaxy at the chip gap (but zero at the edge), and about half as bad in a galaxy one magnitude brighter. Verifying this in practice would require a new survey similar in size to COSMOS (Scoville *et al.* 2007).

Most dramatically, the charge trap density increased  $\sim 80\%$  more than expected between the failure of ACS in January 2007 and its resumption of activities after shuttle Servicing Mission 4. It is not yet clear whether this degradation is related to the decrease in operating temperature, the increase in temperature while ACS was offline, or coincidentally due to the ending of the solar cycle. Our current analysis uses almost all the suitable archival data currently available without yielding conclusive evidence. To resolve this issue, we plan continued monitoring for a further year.

## ACKNOWLEDGMENTS

I would like to thank the CTI working group at STScI, including Linda Smith, Ray Lucas, Pey Lian Lim, Norman Grogin and David Golimowski. I am especially grateful to Jay Anderson who shared his paper before publication. Roger Smith and Alex Short provided physical insight, and Chris Stoughton provided code. Suggestions about temperature effects from the referee proved invaluable: thank you!

The author is supported by STFC Advanced Fellowship #PP/E006450/1 and European Research Council grant MIRG-CT-208994. This work was based on observations with the NASA/ESA *Hubble Space Telescope*, obtained at the Space Telescope Science Institute, which is operated by AURA Inc, under NASA contract NAS 5-26555. Data were used from programmes GO-9075, GO-9822, GO-10092, GO-10496, GO-10896, GO-11563, GO-11600 and GO-11689.

## REFERENCES

- Anderson J. & Bedin L., 2010, PASP in press (arXiv:1007.3987)
- Biretta J. & Kozhurina-Platais V., 2005, Instrument Science Report WFPC2-2005-001
- Bristow P., 2003, Instrument Science Report CE-STIS-2003-001
- Cawley L., Goudfrooij P., Whitmore B., Stiavelli M. & the STScI CTE Working Group, 2002, Instrument Science Report WFC3-2001-005
- Chiaberge M., Lim P. L., Kozhurina-Platais V., Sirianni M. & Mack J., 2009, Instrument Science Report ACS-2009-01
- Hardy T., 1998, IEEE Trans. Nuclear Sci. 45, 154
- Hopkinson G., 2001, IEEE Trans. Nuclear Sci. 48, 6
- Janesick J., “Scientific Charge Coupled Devices”, 2001, SPIE (ISBN 0-8194-3698-4)
- Jones M., 2000, Instrument Science Report ACS-2000-09
- Mack J., Gilliland R., Anderson J., & Sirianni M., 2007, Instrument Science Report CE-ACS-2007-002
- Massey R., Stoughton C., Leauthaud A., Rhodes J., Koekoemoer A., Ellis R. & Shaghoulouian E., 2010, MNRAS 401, 371

- Piatek S. *et al.* 2005, *AJ* 130, 95  
Rhodes J. *et al.*, 2007, *ApJS* 172, 203  
Rhodes J., Leauthaud A., Stoughton C., Massey R., Dawson K., Kolbe W. & Roe N., 2010, *PASP* 122, 439  
Scoville N. *et al.*, 2007, *ApJ* 172, 38  
Short A., Prod'homme T., Weiler M., Brown S. & Brown A., 2010, *Proc. SPIE* 7742, 774212  
Sirianni M., Gilliland R. & Sembach K., 2007, Instrument Science Report CE-ACS-2006-002  
Sirianni M. & Mutchler M., 2006, *Scientific Detectors for Astronomy 2005* (Springer) p. 171, eds. J. Beletic *et al.*